# Use of a Support Vector Machine for Keratoconus and Subclinical Keratoconus Detection by Topographic and Tomographic Data

*Maria Clara Arbelaez, MD,[1] Francesco Versaci, MSE,[2] Gabriele Vestri, MSE,[2] Piero Barboni, MD,[3] Giacomo Savini, MD[4]*

***Purpose:*** To define a new classification method for the diagnosis of keratoconus based on corneal measurements provided by a Scheimpflug camera combined with Placido corneal topography (Sirius, CSO, Florence, Italy).

***Design:*** Retrospective case series.

***Participants:*** We analyzed the examinations of 877 eyes with keratoconus, 426 eyes with subclinical keratoconus, 940 eyes with a history of corneal surgery (defined as abnormal), and 1259 healthy control eyes.

***Methods:*** For each group, eyes were divided into a training and a validation set. A support vector machine (SVM) was used to analyze the corneal measurements and classify the eyes into the 4 groups of participants. The classifier was trained to consider the indices obtained from both the anterior and posterior corneal surfaces or only from the anterior corneal surface.

***Main Outcome Measures:*** Symmetry index of front and back corneal curvature, best fit radius of the front corneal surface, Baiocchi Calossi Versaci front index ($BCV_f$) and BCV back index ($BCV_b$), root mean square of front and back corneal surface higher order aberrations, and thinnest corneal point were analyzed. The diagnostic performance of the classifier was evaluated.

***Results:*** The accuracy of the classifier was excellent both with and without the data generated from the posterior corneal surface and corneal thickness because the number of true predictions was greater than 95% and 93%, respectively, in all classes. Precision improved most when posterior corneal surface data were included, especially in cases of subclinical keratoconus. Using the data from both anterior and posterior corneal surfaces and pachymetry allowed the SVM to increase its sensitivity from 89.3% to 96.0% in abnormal eyes, 92.8% to 95.0% in eyes with keratoconus, 75.2% to 92.0% in eyes with subclinical keratoconus, and 93.1% to 97.2% in normal eyes.

***Conclusions:*** The classification algorithm showed high accuracy, precision, sensitivity, and specificity in discriminating among abnormal eyes, eyes with keratoconus or subclinical keratoconus, and normal eyes. Including the posterior corneal surface and thickness parameters markedly improved the sensitivity in the diagnosis of subclinical keratoconus. Classification may be particularly useful in excluding eyes with early signs of corneal ectasia when screening patients for excimer laser surgery.

***Financial Disclosure(s):*** Proprietary or commercial disclosure may be found after the references.
*Ophthalmology 2012;119:2231–2238 © 2012 by the American Academy of Ophthalmology.*

Keratoconus is a noninflammatory ectatic disease characterized by progressive thinning and steepening and an apical cone-shaped protrusion of the cornea.[1,2] Clinical diagnosis of moderate to advanced keratoconus is not difficult because of the presence of classic retinoscopic and biomicroscopic signs. Identification of early cases with good visual acuity and no specific corneal findings is often challenging, but it is a primary concern when screening patients for refractive surgery because keratoconus is known to weaken the corneal stroma, thus leading to an increased risk of iatrogenic ectasia.[3–7]

Since the introduction of corneal topography, many methods have been suggested for differentiating between normal and keratoconic eyes. Qualitative analysis of color-coded maps enables straightforward pattern recognition of advanced keratoconus, but it is problematic in suspect or early cases, in which it may be biased by subjective interpretation.[8] Therefore, detection schemes have been introduced to enable objective identification of keratoconus. They include quantitative descriptors derived from the analysis of several topographic data, such as the KISA% index proposed by Rabinowitz and Rasheed,[9] the Cone Location


ISSN 0161-6420/12/$–see front matter
http://dx.doi.org/10.1016/j.ophtha.2012.06.005

and Magnitude Index proposed by Mahmoud et al,[10] and the Keratoconus Prediction Index and Keratoconus Index proposed by Maeda et al.[8,11] Alternative automated detection systems have been described by Smolek and Klyce,[12] who developed a classification neural network based on corneal topography indices, Chastang et al,[13] who developed binary decision trees based on corneal topography indices,[1] Twa et al,[14] who developed an automated decision-tree classification of corneal shape through Zernike polynomial analysis, and Maeda et al, who incorporated the Keratoconus Prediction Index into a binary decision tree[8] and later relied on a neural network to classify topographic maps.[11] Other detection schemes based on Zernike decomposition of the anterior corneal surface have been described by Schwiegerling and Greivenkamp[15] (Z3 index) and Langenbucher et al.[16]

More recently, Scheimpflug cameras and slit-scanning corneal topographers have made it possible also to evaluate the posterior corneal surface and corneal thickness. These measurements, which were first reported by Tomidokoro et al in 2000,[17] have been included in new algorithms for the diagnosis of keratoconus. Bessho et al,[18] who used the Orbscan II (Bausch & Lomb, Rochester, NY), proposed an automated keratoconus classifier applying a Fourier-incorporated keratoconus-detection index based on information obtained by Fourier analysis from anterior and posterior corneal surfaces and corneal thickness. With the same technology, Fam and Kim[19] found that anterior corneal elevation parameters had higher sensitivity in detecting keratoconus than posterior corneal elevation, whereas Saad and Gatinel[20] observed that the indices generated from corneal thickness and curvature measurements over the entire cornea can identify forme fruste keratoconus undetected by a Placido-based neural network. Posterior corneal curvature and pachymetric data provided by Scheimpflug imaging have been investigated by Ambrósio et al,[21] who showed that corneal-thickness spatial profile, corneal-volume distribution, percentage increase in thickness, and percentage increase in volume were different in keratoconic and normal eyes. Measurements obtained from the posterior corneal curvature using a Scheimpflug camera have been evaluated in several other articles.[22–24]

The recent introduction of a new Scheimpflug camera combined with Placido disc corneal topography (Sirius, CSO, Florence, Italy), whose software features a machine learning classifier aiming to detect the presence of keratoconus or suspect keratoconus, prompted us to investigate its diagnostic performance. We aimed to describe this method, which is based on the data derived from both anterior and posterior corneal surfaces, and report its accuracy in labeling an eye as abnormal, keratoconus, subclinical keratoconus, or normal relying on classification by support vector machine (SVM), a machine learning technique.

## Materials and Methods

This was a retrospective case series study. Clinical data and corneal examinations were retrieved from clinical records at the Muscat Eye Laser Center (Muscat, Oman) and Studio Oculistico d'Azeglio (Bologna, Italy). The study was conducted in accordance with the ethical standards stated in the 1964 Declaration of Helsinki and approved by the local clinical research ethics committee with informed consent obtained.

### Procedure

Corneal curvature, elevation, and thickness measurements were obtained by means of a Scheimpflug camera combined with Placido corneal topography (Sirius, software version 1.2, CSO, Firenze, Italy). The scanning process acquires a series of 25 Scheimpflug images (meridians) and 1 Placido top view image. The ring edges are detected on the Placido image so that height, slope, and curvature data are calculated using the arc-step method with conic curves. From the Scheimpflug images, the profiles of anterior cornea, posterior cornea, anterior lens, and iris are derived. Anterior surface data from both Placido images and Scheimpflug images are merged using a proprietary method. All the other measurements for internal structures (posterior corneal curvature, anterior lens surface, and iris) are derived solely from Scheimpflug data. Previous studies have reported that the system's pachymetric and shape measurements (curvature, eccentricity, elevation) have good repeatability.[25,26] Measurements were performed by a single experienced examiner in each center according to the manufacturer's guidelines. The examiner was unaware of the clinical diagnosis. The device was brought into focus, and the patient's eye was aligned along the visual axis using a central fixation light. One scan was obtained for each patient. Every examination was critically reviewed for the quality of the topographic and tomographic image, alignment, and anterior and posterior coverage. In case of a poor quality scan, a new scan was repeated, and the patient was excluded if the new scan was also poor quality.

### Patients

On the basis of clinical diagnosis, eyes were classified into the following 4 groups:

1. Those with a clinical diagnosis of keratoconus: Such a diagnosis was established by using a combination of corneal thickness and slit-lamp findings and was confirmed by chart review, applying the criteria established by the Collaborative Longitudinal Evaluation of Keratoconus study.[27] The ocular findings that defined keratoconus included (a) an irregular cornea determined by distorted keratometry mires and distortion of the retinoscopic or ophthalmoscopic red reflex (or a combination of these); and (b) at least 1 of the following biomicroscopic signs: Vogt's striae, Fleischer's ring of greater than 2 mm arc, or corneal scarring consistent with keratoconus. Eyes with a diagnosis of marginal pellucid degeneration were excluded.
2. Those with a diagnosis of subclinical keratoconus: This included patients with a videokeratographic and tomographic pattern of localized steepening in the posterior or anterior corneal surface or paracentral corneal thinning, but no clinical (keratometric, retinoscopic, or biomicroscopic) signs of keratoconus, and with a best-corrected visual acuity of 20/20 or better. This group included eyes with early or forme fruste keratoconus (i.e., eyes of patients with clinically evident keratoconus in the fellow eye) and keratoconus suspects (i.e., corneas with subtle signs of keratoconus but without evidence of clinical keratoconus in either eye), as defined by Klyce.[28]
3. Those with a history of refractive surgery, penetrating keratoplasty, or ocular trauma: This set was defined as abnormal.
4. A sample of normal eyes enrolled among subjects undergoing a routine ophthalmological examination for minor

refractive defects: Exclusion criteria for this group were previous surgery, familial history for keratoconus, contact lens wearing in the last 5 months, and astigmatism >3 diopters.

As previously done by other investigators,[8,10,12,18] each group was divided into a training set (including 200 eyes) to be used to develop the keratoconus detection program and a validation set (including the remaining eyes).

## Support Vector Machine Architecture

Machine learning classifiers aim to define to which category the data of a sample belong. The SVM is a supervised learning technique that can be used for pattern classification.[29–32] The main goal of SVM is to construct, by means of a training set, an optimal hyperplane as the decision surface, in such a way that the margin of separation between the closest data points belonging to different classes is maximized (a hyperplane in an n-dimensional space is the analogue of a plane in 3 dimensions and of a line in 2 dimensions). New data points are then mapped into the same space and predicted to belong to a category on the basis of which side of the gap they fall in. Data points are viewed as n-dimensional vectors, and linear SVMs aim to separate such points with an (n–1)-dimensional hyperplane (n-dimensional plane).

The following indices, based on curvature, thickness, and height data of both the anterior and posterior corneal surface and pachymetry, were used to train the SVM.

## Curvature-based Indices

**Symmetry Index of Front ($SI_f$) and Back Corneal Curvature ($SI_b$).** The symmetry index of front corneal curvature ($SI_f$) was defined as the difference in mean anterior tangential curvature (expressed in diopters) between 2 circular zones centered on the vertical axis in the inferior and superior hemispheres (center: x = 0 mm; y = ±1.5 mm; radius: 1.5 mm).[33] $SI_f$ measures the vertical asymmetry of anterior corneal curvature: Positive values indicate a steeper inferior hemisphere, whereas negative values indicate a steeper superior hemisphere.

Likewise, the symmetry index of back curvature ($SI_b$) was defined as the difference in mean posterior tangential curvature between 2 circular zones centered on the vertical axis in the inferior and superior hemispheres. Because $SI_b$ is measured in diopters and the difference between the refractive index of the cornea and that of the aqueous produces a value of opposite sign relative to $SI_f$ (which is measured on the anterior corneal surface), the arithmetic sign of $SI_b$ was arbitrarily changed to make comparison with $SI_f$ easier.

## Elevation-based Indices

Differences calculated from asphero-toric best fit reference surfaces were used to model the elevation data of anterior and posterior corneal surfaces over a diameter of 8 mm. The asphericity of the reference surface was set equal to the average value in the 8-mm zone, as measured in our sample of normal eyes ($P = 0.78 \pm 0.13$ for the anterior surface, $P = 0.74 \pm 0.18$ for the posterior surface). Elevation data were decomposed into Zernike polynomials up to the 7th order, centered on the corneal vertex, as previously done by Schwiegerling and Greivenkamp.[15]

1. Best-fit radius of the anterior corneal surface ($R^{bf}{}_f$)

The best-fit radius of the anterior surface ($R^{bf}{}_f$) was defined as the measurement (in millimeters) of the apical radius of the best-fit ellipsoid with the eccentricity of an average eye over an 8-mm diameter ($P = 0.8$). The apical radius was calculated for the whole surface because this approach is less influenced by noise and artefacts than calculating the apical radius for a single meridian or a couple of meridians.

2. Baiocchi Calossi Versaci front index ($BCV_f$) and BCV back index ($BCV_b$)

Schwiegerling and Greivenkamp[15] and Li et al[34] have shown that the following coefficients are the most relevant for keratoconus detection: vertical trefoil $c_3{}^{-3}$, vertical coma $c_3{}^{-1}$, horizontal coma $c_3{}^{+1}$, primary spherical aberration $c_4{}^{0}$, and second order vertical coma $c_5{}^{-1}$. The $BCV_f$, which is expressed in micrometers, was obtained by properly combining these coefficients (from the anterior corneal surface) and weighting them by a function of the coma axis. Likewise, a linear combination of $c_3{}^{-3}$, $c_3{}^{-1}$, $c_3{}^{+1}$, $c_4{}^{0}$, and $c_5{}^{-1}$ and information about the coma axis on the posterior Zernike decomposition were used to define the $BCV_b$.

3. Root mean square of higher-order aberrations

On the basis of previous studies showing that higher-order aberrations of the anterior corneal surface can be used as a tool to detect and grade keratoconus,[35,36] we measured the front and back corneal surface root mean square of higher-order aberrations.

## Thickness-based Indices

Because keratoconus is characterized by stromal thinning in the region of the protrusion, an index based on the thinnest value of corneal pachymetry is likely to help in discriminating between normal and keratoconic eyes. The thinnest corneal value was calculated over an 8-mm area.

## Support Vector Machine Training and Test

To optimize the SVM classification, highest and lowest values had to be defined for each parameter. The values equal to the highest and lowest measurements were set as the superior and inferior limits, respectively. In the SVM algorithm, the data of each index were normalized to ±1 using these limits, as suggested by Theodoridis and Koutroumbas[29] and Cristianini and Shawe-Taylor.[30]

The SVM algorithms were implemented by 2 of the authors (F.V., G.V.) using c# programming language in the Microsoft Visual Studio (Microsoft Corp., Redmond, WA) development environment.

To classify a new eye as belonging to 1 of the 4 validation sets, a one-against-one strategy was adopted: This approach involves constructing a machine for each pair of classes resulting in N(N-1)/2 machines, where N is the total number of classes. When applied to a test point, each classification gives 1 vote to the winning class, and the point is labeled with the class having the most votes. By using the described indices derived from both corneal surfaces, 4 sets (N = 4) were used to train 6 SVMs (abnormal vs. keratoconus, abnormal vs. normal, abnormal vs. subclinical keratoconus, keratoconus vs. normal, keratoconus vs. subclinical keratoconus, and normal vs. subclinical keratoconus). The classification provided by the SVM has been shown by the Sirius in the Keratoconus Display (Fig 1) since software version 1.2. The same strategy was then applied when just the anterior corneal surface indices were considered.

## Statistical Analysis

All statistical analyses were performed using MATLAB Statistics Toolbox v.6.5 (MathWorks, Natick, MA) and IBM SPSS v.19 (IBM Corp, Armonk, NY). The normal distribution of each index

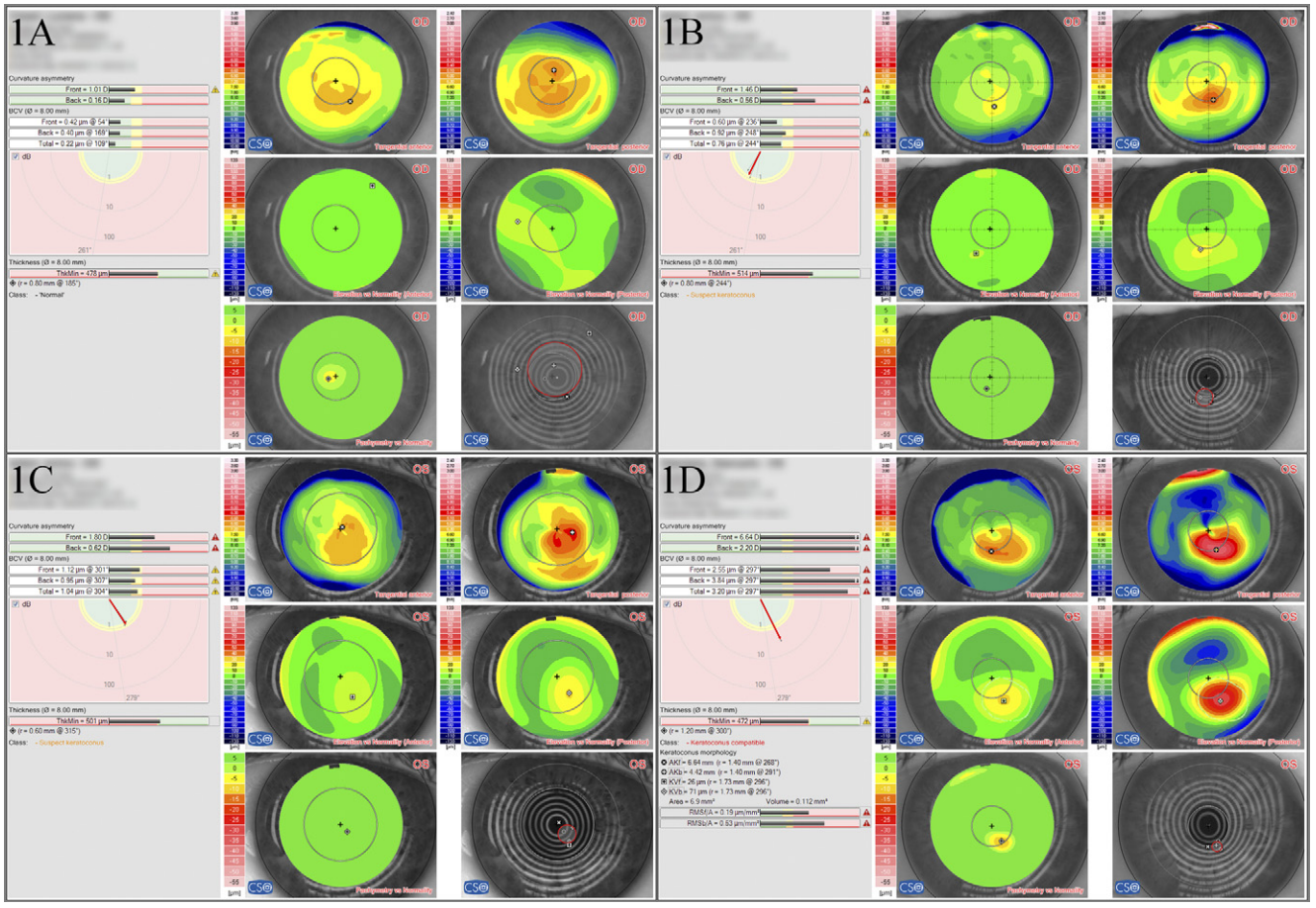


**Figure 1.** Keratoconus screening display, as shown by Sirius. **A,** Normal case with no elevation anomalies but with anterior corneal surface asymmetry and high curvature and with low corneal thickness that may resemble keratoconus. **B,** Keratoconus suspect with slightly skewed astigmatism on the anterior surface and markedly asymmetric curvature and abnormal elevation on the posterior corneal curvature. **C,** Keratoconus suspect with slightly asymmetric curvature and elevation of both corneal surfaces. **D,** Keratoconus with markedly asymmetric curvature and elevation of both corneal surfaces.

in all groups was investigated using the Lilliefors test.[37] Because the distribution of most indices was not Gaussian, the 1st, 5th, 50th, 95th, and 99th percentiles were estimated to provide a descriptive analysis. Statistical differences among groups were assessed for each index by nonparametric analysis of variance (Kruskal–Wallis with Dunn's multiple comparisons test). A confusion matrix (i.e., a contingency table) was used to show the SVM's class predictions compared with the actual outcome in the test data. A $P$ value less than 0.05 was considered statistically significant.

For each continuous random variable, the probability density function (PDF) was computed to describe the relative likelihood of that variable occurring at a given point. For this purpose, the training and validation sets were merged.

## Classification Evaluation Criteria

For each group, precision, sensitivity, specificity, and accuracy of the SVM classification were determined on the basis of the number of true-positive (tp), true-negative (tn), false-positive (fp), and false-negative (fn) cases. Because this was a multiclass predictive model, the following definitions were used for precision, sensitivity, specificity, and accuracy:[38]

1. Accuracy is the overall correctness of the model and is calculated as the sum of correct classifications divided by the total number of classifications, that is, (tp + tn) / (total number of eyes). In a multiclass predictive model, the tn value is calculated as the sum of tn predictions from all columns in the confusion matrix.
2. Precision is a measure of accuracy, provided that a specific class has been predicted. It is defined as tp / (tp + fp), and in a multiclass predictive model, the fp value is calculated as the sum of errors in the column of the confusion matrix.
3. Sensitivity (or tp rate) is a measure of the ability of a prediction model to correctly classify the cases of a given data set and is the result of the ratio tp / (tp + fn).
4. Specificity (or tn rate) is defined as tn / (tn + fp). The tn amount is calculated as the difference between the total amount of cases and (tp + fp + fn).

# Results

Overall, 3502 eyes were enrolled. According to the clinical diagnosis, they were classified as follows:

1. Keratoconus: 877 eyes of 451 patients (mean age, 34.8±12.6 years; range, 15–71 years).
2. Subclinical keratoconus: 426 eyes of 340 patients (mean age, 40.4±17.1 years; range, 15–65 years). This group

Table 2. Confusion Matrix (Actual vs. Predicted Classes), Accuracy, Precision, Sensitivity, and Specificity of the Support Vector Machine Classification Performed on the Validation Set, Based on Anterior and Posterior Corneal Surfaces and Pachymetry Data

| | | Predicted Classes | | | | | | | |
|---|---|---|---|---|---|---|---|---|---|
| **Actual Classes** | **N** | *Abnormal* | *Keratoconus* | *Subclinical Keratoconus* | *Normal* | **Accuracy** | **Precision** | **Sensitivity** | **Specificity** |
| Abnormal | 740 | 712 | 6 | 8 | 14 | 98.3% | 97.4% | 96.2% | 99.0% |
| Keratoconus | 677 | 7 | 643 | 27 | 0 | 98.2% | 97.9% | 95.0% | 99.3% |
| Subclinical keratoconus | 226 | 3 | 8 | 208 | 7 | 97.3% | 78.8% | 92.0% | 97.7% |
| Normal | 1059 | 9 | 0 | 21 | 1029 | 98.1% | 98.0% | 97.2% | 98.7% |

included 229 eyes with early keratoconus and 197 eyes with suspect keratoconus.

3. Abnormal: 940 eyes of 486 patients (mean age, 43.6±13.6 years; range, 14–78 years).
4. Normal: 1259 eyes of 756 normal patients (mean age, 39.3±16.2 years; range, 16–77 years). Among normal eyes, 216 eyes (37 in the training set and 179 in the validation set) showed some suspect topographic or tomographic data.

Table 1 (available at http://aaojournal.org) shows the results of the Lilliefors test for normality and the descriptive statistic for each index and for each group. Only a few of the examined indices were normally distributed. Nonparametric analysis of variance detected statistically significant differences ($P<0.001$) among the 4 groups for each index, the only exception being the post-test between the $R^{bf}_f$ of the normal and subclinical keratoconus groups.

Histograms in Figures 2 and 3 (available at http://aaojournal.org) show an approximation of the PDF for $SI_f$ and $SI_b$ continuous random variables for each group and reveal that an asymmetric inferior corneal steepening was evident on both surfaces in eyes with suspect keratoconus and, to a higher extent, in eyes with keratoconus. Figure 4 (available at http://aaojournal.org) shows the PDF of $R^{bf}_f$ and reveals lower values in keratoconic eyes compared with normal eyes and keratoconus suspects (a wide range of values are present in the abnormal set). Figures 5 and 6 (available at http://aaojournal.org) show the PDFs of $BCV_f$ and $BCV_b$, and reveal that these indices were higher in the keratoconus group compared with the other groups of eyes. Figures 7 and 8 (available at http://aaojournal.org) show the PDFs of the front and back corneal surface root mean square, and reveal higher values in the abnormal and keratoconus groups and a smaller separation between normal eyes and keratoconus suspects. Figure 9 (available at http://aaojournal.org) represents the PDF of the thinnest corneal value and reveals lower pachymetric values in keratoconic eyes and keratoconus suspects compared with normal eyes, in addition to a wide range of variability for the values in the abnormal set.

## Classification

The confusion matrix and the results of the SVM classifier considering both the anterior and the posterior surface–based indices and the pachymetry indices are presented in Table 2; the results of the SVM classifier considering only the anterior surface–based indices are shown in Table 3. The accuracy of the SVM classifier was excellent with (Table 2) and without (Table 3) the data generated from the posterior corneal surface and corneal thickness because the number of true predictions (= tp + tn) was always more than 97% and 93%, respectively.

Precision was most affected when posterior corneal surface data were omitted, especially in the case of subclinical keratoconus, in which the number of false-positives decreased from 126 to 56 when both corneal surfaces were considered. Precision increased accordingly from 57.4% to 78.8% when posterior corneal surface data were included in the analysis. The rate of success in differentiating keratoconic from normal eyes did not depend on the measurements of the posterior corneal surface. No eye in the normal set was classified as keratoconic and no eye in the keratoconus set was classified as normal when the data of the whole cornea were taken into account (Table 2). Likewise, no eye in the normal set was classified as keratoconic, and just 1 eye of 677 (0.1%) in the keratoconus set was classified as normal when only anterior videokeratographic data were taken into account (Table 3).

Sensitivity was higher when both corneal surfaces were analyzed. Including the posterior corneal curvature and pachymetric data increased the sensitivity in the diagnosis of abnormal eyes (from 89.3% to 96.2%), keratoconus (from 92.8% to 95.0%), subclinical keratoconus (from 75.2% to 92.0%), and normal eyes (from 93.1% to 97.2%).

Specificity was less influenced by the inclusion or omission of posterior corneal curvature and pachymetric data, although a slight reduction in specificity was observed in all classes when only the anterior corneal surface was analyzed.

# Discussion

Preoperative screening of patients undergoing corneal refractive surgery requires correct identification of eyes with subclinical keratoconus because subjects with this condition are known to be at increased risk of developing iatrogenic ectasia.[3–7] When no signs of keratoconus are detected in

Table 3. Confusion Matrix (Actual vs. Predicted Classes), Accuracy, Precision, Sensitivity, and Specificity of the Support Vector Machine Classification Performed on the Validation Set, Based on Only Anterior Corneal Surface Data

| | | Predicted Classes | | | | | | | |
|---|---|---|---|---|---|---|---|---|---|
| **Actual Classes** | **N** | *Abnormal* | *Keratoconus* | *Subclinical Keratoconus* | *Normal* | **Accuracy** | **Precision** | **Sensitivity** | **Specificity** |
| Abnormal | 740 | 661 | 31 | 27 | 21 | 96.0% | 95.8% | 89.3% | 98.5% |
| Keratoconus | 677 | 6 | 628 | 42 | 1 | 96.9% | 94.6% | 92.8% | 98.2% |
| Subclinical keratoconus | 226 | 7 | 5 | 170 | 44 | 93.3% | 57.4% | 75.2% | 94.9% |
| Normal | 1059 | 16 | 0 | 57 | 986 | 94.9% | 93.7% | 93.1% | 96.0% |

either eye, this task represents a challenge for the ophthalmologist, given the lack—by definition—of any clinical difference between normal eyes and eyes with subclinical keratoconus. The only current way to diagnose the latter condition is by means of corneal topography or tomography; however, the indices provided by these technologies frequently show overlapping values between the 2 categories of eyes, so that it is difficult to find a clear cutoff value and use a single parameter for the differential diagnosis.[17,20,39] Qualitative analysis by subjective pattern recognition is obviously biased by personal experience. A possible solution to this problem is given by machine learning, that is, algorithms that automatically and objectively classify an eye as belonging to a category, based on a combination of topographic and tomographic corneal measurements.

The present study shows that applying SVM, a machine learning technique, to the corneal measurements provided by the Sirius, a Scheimpflug camera combined with a Placido disc corneal topographer, can accurately classify eyes as belonging to the category of normal, keratoconus, subclinical keratoconus, or abnormal. Analysis of only the anterior corneal surface parameters may be sufficient to discriminate between normal eyes and eyes with clinical keratoconus. Using the data from both corneal surfaces increases the precision, sensitivity, specificity, and accuracy of the SVM classifier and significantly improves the ability to differentiate between normal eyes and subclinical keratoconus suspects. This result is in good agreement with the substantial evidence suggesting that early morphologic changes in eyes with keratoconus may be present not only on the anterior corneal surface but also on the posterior surface,[17,39] and several studies have already emphasized the clinical relevance of posterior corneal curvature and pachymetric data in the diagnosis of keratoconus.[17,20,21,23,40] Tables 2 and 3 show that the use of posterior and pachymetric data is crucial in the detection of subclinical keratoconus because 92% of these eyes were correctly classified when the posterior corneal and pachymetric measurements were considered, compared with only 75.2% when just the anterior corneal surface was evaluated. When both corneal surfaces were considered, only 3.1% of eyes with subclinical keratoconus were classified as normal (Table 2) and 3.5% as keratoconic. Of note, sensitivity was similar for the 2 subcategories of subclinical keratoconus (data not shown in Table 2): In the validation set, 94 eyes of 104 with forme fruste keratoconus (sensitivity = 92.0%) and 112 eyes of 122 with suspect keratoconus (sensitivity = 91.8%) were correctly classified.

Machine learning tools have already been used for the diagnosis of keratoconus. Maeda et al[8] used an expert system classifier (combining a discriminant analysis and a classification tree) to analyze the data of Placido ring–based corneal topography. They found a sensitivity of 89% in discriminating keratoconic from normal eyes: This is lower than the value we achieved with SVM based on both corneal surfaces and pachymetric data (95%) and closer to that achieved by anterior corneal surface analysis (92%). However, a direct comparison between the results of Maeda et al and our own study is not possible because they did not include subclinical keratoconus. Smolek and Klyce[12] evaluated a neural network approach for detecting and classifying keratoconus and suspect keratoconus when confronted with a variety of potentially confounding topographic patterns of the anterior corneal surface generated by Placido ring–based corneal topography. They enrolled 150 eyes for both the training and validation sets and subdivided them into 9 groups. They achieved 100% sensitivity and 100% specificity in both keratoconic eyes and keratoconus suspects. These values are slightly better than those obtained in the present study, but again a direct comparison cannot be performed because the sample size is different; the number of eyes with keratonus and keratoconus suspects in their validation set were 33 and 6 versus 677 and 226, respectively, in our study. Twa et al[14] modeled the anterior corneal surface with a seventh-order Zernike polynomial and applied a decision tree classifier to differentiate between normal and keratoconic eyes (subclinical keratoconus was not included in their sample). The sensitivity, specificity, and accuracy of their method were 92%, 93%, and 93% lower, respectively, than our own values.[14] Lower values of sensitivity (88.5%) and specificity (94.5%) were also reported by Chastang et al,[13] who used a binary decision tree based on the data generated by Placido ring–based corneal topography; their study likewise did not include subclinical keratoconus.

Saad and Gatinel[20] performed a discriminant analysis on 72 normal eyes, 40 eyes with forme fruste keratoconus, and 31 eyes affected by keratoconus based on several indices obtained from the anterior and posterior corneal surface and from corneal thickness as measured by the Orbscan IIz (Bausch & Lomb). Their best discriminant function was able to differentiate normal from keratoconic eyes with a sensitivity of 97%, a specificity of 100%, and an accuracy of 99% and normal eyes from forme fruste keratoconic eyes with a sensitivity of 93%, a specificity of 92%, and an accuracy of 92%.[20] These values are similar to those reported in the present study; however, it should be observed that Saad and Gatinel did not validate their method on a separate set as we did in this study.

Overall, the data of this study show a higher diagnostic accuracy of the SVM classifier included in the Sirius compared with previous machine learning techniques. Sensitivity, specificity, and accuracy in the detection of clinical and subclinical keratoconus are higher also in comparison with the methods relying on a single predictive index, although direct comparisons are often not possible. The Fourier-incorporated keratoconus-detection index developed by Bessho et al,[18] for example, yielded sensitivity, specificity, and accuracy values of 96.9%, 95.4%, and 95.9%, respectively, for the diagnosis of keratoconus, but that study included only a few keratoconus suspects (n = 11) and merged them to cases of clinical keratoconus, so that information about the diagnostic performance with respect to keratoconus suspects was not available. Likewise, the Cone Location and Magnitude Index has been tested with excellent results on keratoconic eyes, but it has not been evaluated in subclinical keratoconus.[10] The diagnostic performance of KISA has been found to be modest for suspected keratoconus.[34] Some authors have reported better results

when relying on posterior corneal elevation measurements, with a sensitivity of 68% and specificity of 90.8% being achieved in the diagnosis of subclinical keratoconus.[23]

Comparison with the keratoconus screening software of other Scheimpflug cameras is not possible. The diagnostic performance of the Belin-Ambrosio Enhanced Ectasia display of the Pentacam (Oculus Optikgeräte GmbH, Wetzlar, Germany) has never been tested to our knowledge. By using this device, Ambrósio et al[41] compared 44 eyes with keratonus and 113 normal patients and found that the pachymetric progression indices were better able to differentiate the 2 samples of patients, but their analysis did not include subclinical keratoconus and did not evaluate corneal curvature data. Similar results, involving also anterior and posterior elevation data, were reported by Miháltz et al.[42] Uçakhan et al[22] analyzed several Pentacam indices (based on both corneal surfaces, curvature elevation and corneal thickness) in normal eyes and patients with subclinical keratoconus and clinically evident keratoconus. They found that a combination of corneal power, thickness, and anterior elevation parameters was best in discriminating keratoconus eyes from normal eyes, whereas a combination of corneal power, thickness, and posterior elevation parameters was best in discriminating subclinical keratoconus eyes from normal eyes. However, these models are not available on the commercially available Pentacam. The current software version of the Galilei (Ziemer Ophthalmics, Port, Switzerland) does not include a specific analysis for keratoconus diagnosis, whereas the keratoconus screening software of the TMS-5 (Tomey Corp, Tokyo, Japan) does not take into account posterior corneal surface and pachymetric measurements.

This study is limited by its retrospective design. Although we already validated the diagnostic performance by means of a training and a validation set, it would be reassuring to have our data confirmed by a prospective investigation.

In conclusion, the present study shows that an SVM-based algorithm can be successfully used to differentiate normal eyes from eyes with clinical and subclinical keratoconus. The diagnostic accuracy of the SVM classifier is further improved by including measurements of the posterior corneal surface and corneal thickness. This tool can help clinicians in detecting eyes with subclinical keratoconus in preoperative screening for refractive surgery.

## References


1. Rabinowitz YS. Keratoconus. Surv Ophthalmol 1998;42:297–319.
2. Krachmer JH, Feder RS, Belin MW. Keratoconus and related noninflammatory corneal thinning disorders. Surv Ophthalmol 1994;28:293–322.
3. Ambrosio R Jr, Wilson SE. Complications of laser in situ keratomileusis: etiology, prevention, and treatment. J Refract Surg 2001;17:350–79.
4. Binder PS. Analysis of ectasia after laser in situ keratomileusis: risk factors. J Cataract Refract Surg 2007;33:1530–8.
5. Binder PS. Risk factors for ectasia after LASIK [letter]. J Cataract Refract Surg 2008;34:2010–1.
6. Randleman JB, Trattler WB, Stulting RD. Validation of the Ectasia Risk Score System for preoperative laser in situ keratomileusis screening. Am J Ophthalmol 2008;145:813–8.
7. Randleman JB, Woodward M, Lynn MJ, Stulting RD. Risk assessment for ectasia after corneal refractive surgery. Ophthalmology 2008;115:37–50.
8. Maeda N, Klyce SD, Smolek MK, Thompson HW. Automated keratoconus screening with corneal topography analysis. Invest Ophthalmol Vis Sci 1994;35:2749–57.
9. Rabinowitz YS, Rasheed K. KISA% index: a quantitative videokeratography algorithm embodying minimal topographic criteria for diagnosing keratoconus. J Cataract Refract Surg 1999;25:1327–35.
10. Mahmoud AM, Roberts CJ, Lembach RG, et al, CLEK Study Group. CLMI: the Cone Location and Magnitude Index. Cornea 2008;27:480–7.
11. Maeda N, Klyce SD, Smolek MK. Neural network classification of corneal topography: preliminary demonstration. Invest Ophthalmol Vis Sci 1995;36:1327–35.
12. Smolek MK, Klyce SD. Current keratoconus detection methods compared with a neural network approach. Invest Ophthalmol Vis Sci 1997;38:2290–9.
13. Chastang PJ, Borderie VM, Carvajal-Gonzalez S, et al. Automated keratoconus detection using the EyeSys videokeratoscope. J Cataract Refract Surg 2000;26:675–83.
14. Twa MD, Parthasarathy S, Roberts C, et al. Automated decision tree classification of corneal shape. Optom Vis Sci 2005;82:1038–46.
15. Schwiegerling J, Greivenkamp JE. Keratoconus detection based on videokeratoscopic height data. Optom Vis Sci 1996;73:721–8.
16. Langenbucher A, Gusek-Schneider GC, Kus MM, et al. Keratoconus screening with wave-front parameters based on topography height data [in German]. Klin Monbl Augenheilkd 1999;214:217–23.
17. Tomidokoro A, Oshika T, Amano S, et al. Changes in anterior and posterior corneal curvatures in keratoconus. Ophthalmology 2000;107:1328–32.
18. Bessho K, Maeda N, Kuroda T, et al. Automated keratoconus detection using height data of anterior and posterior corneal surfaces. Jpn J Ophthalmol 2006;50:409–16.
19. Fam HB, Lim KL. Corneal elevation indices in normal and keratoconic eyes. J Cataract Refract Surg 2006;32:1281–7.
20. Saad A, Gatinel D. Topographic and tomographic properties of forme fruste keratoconus corneas. Invest Ophthalmol Vis Sci 2010;51:5546–54.
21. Ambrósio R Jr, Alonso RS, Luz A, Coca Velarde LG. Corneal-thickness spatial profile and corneal-volume distribution: tomographic indices to detect keratoconus. J Cataract Refract Surg 2006;32:1851–9.
22. Uçakhan ÖÖ, Çetinkor V, Özkan M, Kanpolat A. Evaluation of Scheimpflug imaging parameters in subclinical keratoconus, keratoconus, and normal eyes. J Cataract Refract Surg 2011;37:1116–24.
23. de Sanctis U, Loiacono C, Richiardi L, et al. Sensitivity and specificity of posterior corneal elevation measured by Pentacam in discriminating keratoconus/subclinical keratoconus. Ophthalmol 2008;115:1534–9.
24. Piñero DP, Alió JL, Alesón A, et al. Corneal volume, pachymetry, and correlation of anterior and posterior corneal shape in subclinical and different stages of clinical keratoconus. J Cataract Refract Surg 2010;36:814–25.
25. Milla M, Piñero DP, Amparo F, Alió JL. Pachymetric measurements with a new Scheimpflug photography–based

system: intraobserver repeatability and agreement with optical coherence tomography pachymetry. J Cataract Refract Surg 2011;37:310–6.
26. Savini G, Barboni P, Carbonelli M, Hoffer KJ. Repeatability of automatic measurements by a new Scheimpflug camera combined to Placido topography. J Cataract Refract Surg 2011;37:1809–16.
27. Zadnik K, Barr JT, Edrington TB, et al. Collaborative Longitudinal Evaluation of Keratoconus (CLEK) Study Group. Baseline findings in the Collaborative Longitudinal Evaluation of Keratoconus (CLEK) Study. Invest Ophthalmol Vis Sci 1998;39:2537–46.
28. Klyce SD. Chasing the suspect: keratoconus. Br J Ophthalmol 2009;93:845–7.
29. Theodoridis S, Koutroumbas K. Pattern Recognition. 4th ed. Amsterdam: Academic Press; 2009:91–147.
30. Cristianini N, Shawe-Taylor J. An Introduction to Support Vector Machines and Other Kernel-Based Learning Methods. Cambridge: Cambridge University Press; 2000:93–121.
31. Cortes C, Vapnik V. Support-vector networks. Mach Learn 1995;20:273–97.
32. Hsu CW, Chang CC, Lin CJ. A Practical Guide to Support Vector Classification. 2003. Technical report. Taiwan: Department of Computer Science, National Taiwan University. Available at: http://www.csie.ntu.edu.tw/~cjlin/papers/guide/guide.pdf. Accessed May 20, 2012.
33. Calossi A. Screening by computerized videokeratography [in Italian]. In: Il Cheratocono. Canelli, Italy: SOI Publ. Group, Fabiano Group, Ltd; 2004:114–7.
34. Li X, Yang H, Rabinowitz YS. Keratoconus: classification scheme based on videokeratography and clinical signs. J Cataract Refract Surg 2009;35:1597–603.
35. Alió JL, Shabayek MH. Corneal higher order aberrations: a method to grade keratoconus. J Refract Surg 2006;22:539–45.
36. Bühren J, Kühne J, Kohnen T. Defining subclinical keratoconus using corneal first-surface higher-order aberrations. Am J Ophthalmol 2007;143:381–9.
37. Lilliefors HW. On the Kolmogorov–Smirnov test for normality with mean and variance unknown. J Am Stat Assoc 1967; 62:399–402.
38. Altman DG, Bland JM. Diagnostic tests. 1: Sensitivity and specificity. BMJ 1994;308:1552.
39. Rao SN, Raviv T, Majmudar PA, Epstein RJ. Role of Orbscan II in screening keratoconus suspects before refractive corneal surgery. Ophthalmology 2002;109:1642–6.
40. Belin MW, Khachikian SS. Keratoconus: it is hard to define, but . . . Am J Ophthalmol 2007;143:500–3.
41. Ambrósio R Jr, Caiado AL, Guerra FP, et al. Novel pachymetric parameters based on corneal tomography for diagnosing keratoconus. J Refract Surg 2011;27:753–8.
42. Miháltz K, Kovács I, Takács A, Nagy ZZ. Evaluation of keratometric, pachymetric, and elevation parameters of keratoconic corneas with Pentacam. Cornea 2009;28:976–80.

## Footnotes and Financial Disclosures

Originally received: January 16, 2012.
Final revision: April 3, 2012.
Accepted: June 5, 2012.
Available online: August 11, 2012. Manuscript no. 2012-78.

[1] Muscat Eye Laser Center, Muscat, Oman.

[2] CSO srl, Florence, Italy.

[3] Studio Oculistico D'Azeglio, Bologna, Italy.

[4] G.B. Bietti Foundation IRCCS, Rome, Italy.

Financial Disclosure(s):
The author(s) have made the following disclosure(s):

Francesco Versaci and Gabriele Vestri are employees of CSO srl.

Correspondence:
Francesco Versaci, MSE, Via degli Stagnacci 12/E, 50010, Badia a Settimo, Firenze, Italy. E-mail: f.versaci@csoitalia.it.